THE JOURNAL OF BIOLOGICAL CHEMISTRY VOL. 281, NO. 35, pp. 25541–25550, September 1, 2006

The Heme Transfer from the Soluble HasA Hemophore to Its Membrane-bound Receptor HasR Is Driven by Protein-Protein Interaction from a High to a Lower Affinity Binding Site*[S]

Received for publication, April 18, 2006, and in revised form, June 9, 2006 Published, JBC Papers in Press, June 14, 2006, DOI 10.1074/jbc.M603698200

Nadia Izadi-Pruneyre[‡], Frédéric Huché[§1], Gudrun S. Lukat-Rodgers[¶], Anne Lecroisey[‡], Robert Gilli[‖], Kenton R. Rodgers[¶], Cécile Wandersman[§], and Philippe Delepelaire[§2]

From the [§]Unité des Membranes Bactériennes, CNRS URA 2172 Département de Microbiologie and [‡]Unité de Résonance Magnétique Nucléaire des Biomolécules CNRS URA 2185 Département de Biologie Structurale et de la Chimie, Institut Pasteur, 75724 Paris Cedex 15 France, [‖]CNRS FRE 2737, Université de la Méditerranée (Aix-Marseille II), Faculté de Pharmacie 13385 Marseille Cedex 05 France, and [¶]Department of Chemistry, Biochemistry, and Molecular Biology, North Dakota State University, Fargo, North Dakota 58105-5516

HasA is an extracellular heme binding protein, and HasR is an outer membrane receptor protein from *Serratia marcescens*. They are the initial partners of a heme internalization system allowing *S. marcescens* to scavenge heme at very low concentrations due to the very high affinity of HasA for heme (K_a = 5,3 × 10^{10} M^{-1}). Heme is then transferred to HasR, which has a lower affinity for heme. The mechanism of the heme transfer between HasA and HasR is largely unknown. HasR has been overexpressed and purified in holo and apo forms. It binds one heme molecule with a K_a of 5 × 10^6 M^{-1} and shows the characteristic absorbance spectrum of a low spin heme iron. Both holoHasA and apoHasA bind tightly to apoHasR in a 1:1 stoichiometry. In this study we show that heme transfer occurs *in vitro* in the purified HasA·HasR complex, demonstrating that heme transfer is energy- and TonB complex-independent and driven by a protein-protein interaction. We also show that heme binding to HasR involves two conserved histidine residues.

Heme is a key component of many biochemical reactions. These range from electron transfer in cytochromes to oxygen binding in hemoglobin. Due to the toxicity of free heme, it is almost always associated with proteins in living cells. Heme is also a major source of iron for pathogenic or commensal bacteria in mammals (1). Bacteria have developed many strategies for acquiring iron from their surroundings. Gram-negative bacteria rely on specific outer membrane receptors. These are either specific for host heme/iron proteins (heme/hemopexin, hemoglobin, transferrin, lactoferrin) or for very potent iron chelators (siderophores), made in most cases by the bacterium (2). The bacteria may also use a secreted heme-binding protein or hemophore, HasA (3). This system is found in *Serratia marcescens* and several other Gram-negative bacteria. It allows a very efficient heme uptake due to the very high affinity of HasA for heme ($K_a = 5.3 \times 10^{10}$ M^{-1}) (4) and the equally strong apparent affinity *in vivo* of HasA for the HasR receptor (apparent K_d of 5×10^{-9} M) (5). HasA protein contains 188 amino acid residues with a unique folding pattern consisting of a strongly twisted β-sheet (seven strands) on one side of the protein and four α-helices on the other (6). The affinity of HasA for heme is due to two axial heme iron ligands (His-32 and Tyr-75) and a third residue (His-83) stabilizing the Tyr-75-Fe bond (4). The binding of HasA to the HasR receptor depends on two β strands making independent contact with the receptor (7). The HasR receptor belongs to the TonB-class outer membrane-dependent receptors. The three-dimensional structures of these receptors are organized in a "plug and barrel" motif (2). Homology modeling of HasR, based on structural and sequential alignments with receptors of known structure, is consistent with HasR having the same organization (8). Heme receptors have several conserved features; two conserved histidine residues and a so-called FRAP box (9). HasR has similar features, with two conserved histidine residues that are close to each other, as shown by the model; one at the apex of the "plug" and the other one on an extracellular loop (8). Mutations of these conserved residues have been shown to be deleterious in the heme receptor HemR in *Yersinia enterocolitica* (9). The HasR receptor can use different substrates, either free heme up to a concentration of 10^{-6} M or the heme-HasA complex. The system is more efficient for the heme-HasA complex, allowing growth at a heme concentration 100 times lower than for free heme (10). For both substrates heme transport depends upon turnover of the inner membrane TonB·ExbBD protein complex and the proton motive force across the cytoplasmic membrane. Higher concentrations of the TonB complex and greater proton motive force are required for heme uptake involving HasA than for uptake of free heme (11). The precise cascade of events that includes recognition of the hemophore by the receptor, internalization of heme, and release of the empty hemophore is not

* This work was supported in part by NCRR Grant P20 RR15556 and United States Department of Agriculture Grant ND05299 (to K. R. R.). The costs of publication of this article were defrayed in part by the payment of page charges. This article must therefore be hereby marked "*advertisement*" in accordance with 18 U.S.C. Section 1734 solely to indicate this fact.

[S] The on-line version of this article (available at http://www.jbc.org) contains supplemental Table S1.

[1] Supported by a fellowship from the Fondation pour la Recherche Médicale.

[2] To whom correspondence should be addressed: Unité des Membranes Bactériennes, Département de Microbiologie, Institut Pasteur, 25–28, rue du Dr. Roux, 75724 Paris Cedex 15 France. Tel.: 33-1-40-61-32-76; Fax: 33-1-45-68-87-90; E-mail: pdelep@pasteur.fr.

precisely known. Our *in vivo* studies have clearly shown that heme transport is dependent upon the TonB complex and the pmf and that hemophore recycling is also dependent upon the TonB complex and the pmf. However, it is not known whether the TonB complex is required for transfer of the heme from the heme-loaded hemophore to the apo-receptor. We have also shown that recycling of HasA requires heme and a higher TonB complex concentration and pmf than uptake of free heme. *In vivo*, the HasA·HasR complex is irreversible in the absence of an energy source, the TonB complex, and of heme (5).

In the current study the first steps of heme acquisition, the binding of the receptor to its various partners (heme, apo- and holoHasA) and the transfer of heme from the hemophore to the receptor, have been investigated. We have shown that heme transfer from the holohemophore to the aporeceptor does not require the TonB complex and that protein-protein interactions between HasA and HasR drive the heme transfer. Furthermore, we have shown that heme binding to HasR involves two conserved histidine residues.

MATERIALS AND METHODS

Strains, Plasmids, and Growth Conditions—Plasmids pFR2, pFR2H1, pFR2H2, and pFR2H1H2 were pBAD24 derivatives used for expressing WT[3] and histidine mutant HasR receptors under arabinose control. HisHasA was produced as described from pQE32 (8). HasA76t and HasA encoded by pAM derivatives were used to transform a strain carrying a compatible plasmid that encoded secretion functions, allowing purification from the supernatant. HasA76t is a HasA derivative bearing a pentapeptide insertion after residue 76 (7). Popc4420 (a OmpF−OmpC−LamB− derivative of MC4100) was provided by R. Benz and was used for receptor expression. PAP105 was used for HisHasA expression, and MC4100 was for HasA production. Popc4420 derivatives were grown at 30 °C in M9 minimal medium containing glycerol (0.4%), casamino acids (0.2%), 50 μM $FeSO_4$, and 50 μM sodium citrate in 16-liter fermentors. When the cells reached an optical density of 0.7 at 600 nm, arabinose (40 mg/liter) was added, and the cultures incubated for 3 h to induce receptor expression. C600Δ*hemA* and C600Δ*hemAexbBD*::*Tn10* transformed with the various HasR constructs were used for growth tests with exogenous heme-loaded hemophore, heme, and hemoglobin, as previously described (7); for those experiments, HasA variants were used at a 80% heme charge at 40 and 4 μM, and HasR expression was induced by arabinose (20 mg/liter).

Plasmid Construction—PFR2H1 and pFR2H2 were constructed using pFR2 as a template in a mutagenic PCR using the following complementary mutagenic oligonucleotides: Hasrhis1, TTCAAAAGAGCGGCGCTGGCCAACGTAATG; Hasrhis1r, CATTACGTTGGCCAGCGCCGCTCTTTTGAA; Hasrhis2mod, ACCAACGGCAGCGCGGCCAGTTCTTCCACG; Hasrhis2rmod, CGTGGAAGAACTGGCCGCGCTGCCGTTGGT. The mutation was verified by sequencing and reintroduced into an otherwise WT pFR2 plasmid using EcoRI and BsrGI for H1 and BstZ17I and BsiWI for H2. For the construction of the double H1H2 mutant, the EcoRI-BsrGI fragment from pFR2H1 was exchanged for the same fragment from pFR2H2 and yielded pFR2H1H2.

Protein Expression and Purification, Biochemical Techniques—HisHasA was purified as previously described (7) with the following modifications. HisHasA from a soluble fraction of a 500-ml culture was loaded on a Q-Sepharose column (10 ml) and eluted with a 0 to 1 M NaCl gradient in 50 mM Tris-HCl at pH 7.5, allowing for separation of heme-loaded from heme-free protein. The heme-free protein-containing fractions were then combined and loaded on Ni-NTA-agarose and eluted with an imidazole gradient. This yielded pure apoHisHasA, which was purified using size exclusion chromatography. ApoHis-HasA could be loaded with heme using the theoretical molar extinction coefficient for His-HasA of 21,350 $M^{-1}cm^{-1}$ at 276 nm.

ApoHasA WT was purified from cells grown in M9 minimal medium as previously described (12). ApoHasA76t and the heme pocket mutants were purified from a culture supernatant of *Escherichia coli* MC4100 harboring the relevant plasmids (grown in LB at 30 °C) by anion exchange chromatography followed by size exclusion chromatography.

Wild-type and mutant HasR were partially purified from crude membrane preparations obtained after French press treatment; membranes from 50 g of wet cells were resuspended and solubilized in 200 ml of 50 mM Tris-HCl at pH 7.5, 1% ZW3-14 (*n*-tetradecyl-*N*,*N*-dimethyl-3-ammonio-1-propanesulfonate; Calbiochem), 5 mM $MgCl_2$, and protease inhibitors (Roche Applied Science mixture, EDTA free). After 1 h of incubation at 4 °C, the suspension was centrifuged (50,000 × *g* for 1 h). The supernatant, which mostly contained inner membrane proteins, was discarded, and the pellet was resuspended in the same volume of 50 mM Tris-HCl at pH 7.5, 2% ZW3-14, 20 mM EDTA, and protease inhibitors. After 1 h of incubation at 4 °C, the suspension was centrifuged (50,000 × *g* for 1 h), and the supernatant was frozen at 77 K in liquid nitrogen. The pellet was resuspended in the same volume of 50 mM Tris-HCl at pH 7.5, 2.5% ZW3-14, 20 mM EDTA, and protease inhibitors. After 1 h of incubation at 4 °C, the suspension was centrifuged (50,000 × *g* for 1 h), and the supernatant was frozen at 77 K in liquid nitrogen. The combined supernatants from the second and third solubilization were loaded at 2 ml/min on a 20-ml Q-Sepharose fast-flow column equilibrated with buffer A (50 mM Tris-HCl at pH 7.5, 0.02% ZW3-14, 20 mM EDTA) and extensively washed with the same buffer. The bound proteins were then eluted with 20 column volumes of a linear gradient of buffer A and buffer B (50 mM Tris-HCl at pH 7.5, 0.02% ZW3-14, 1 M NaCl) at a flow rate of 2 ml/min at 15 °C. The fractions (4 ml) were tested for the presence of the receptor. and the most enriched fractions were combined and concentrated on an Amicon centriflow filter (cutoff molecular mass of 100 kDa). A second purification by chromatography under the same conditions (but without EDTA) was carried out, and the concentrated fractions were purified on a size exclusion column (Superdex 200pg 320-ml column

[3] The abbreviations used are: WT, wild type; Ni-NTA, nickel-nitrilotriacetic acid; rR, resonance Raman; ITC, isothermal titration calorimetry; ZW3-14, (*n*-tetradecyl-*N*,*N*-dimethyl-3-ammonio-1-propanesulfonate).

60 × 2.6 or Superose 6 24-ml column 300/10; Amersham Biosciences) in 25 mM Tris-HCl at pH 7.5, 0.02% ZW3-14, 150 mM NaCl. The routine yield was about 10 mg of purified HasR from 10 g of cells. For purification of the holo receptor, hemin (10^{-5} M) was added either to the culture 1 h before harvesting or to the membrane preparation before detergent extraction. HoloHasR eluted at a higher salt concentration than for apoHasR for the anion exchange chromatography (not shown).

Complexes of apoHisHasA and apoHasR were purified; an excess of apoHisHasA resuspended in 25 mM Tris-HCl at pH 7.5, 0.02% ZW3-14, 150 mM NaCl was mixed with partially purified apoHasR in the same buffer. After 1 h of incubation at 4 °C, the preparation was mixed with Ni-NTA-agarose in the same buffer and incubated for a further hour. Unbound material was washed with the same buffer containing 20 mM imidazole. Bound material was eluted with the same buffer containing 0.5 M imidazole. The resulting concentrated imidazole eluate was purified on a size exclusion column (Superose 6, 24 ml, 0.5-ml fractions were collected). Control experiments showed that apoHasR did not bind to the Ni-NTA affinity resin under these same conditions (not shown). Absorption spectra (UV-visible) were recorded on a Beckman DU-800 spectrophotometer with 1 cm optical path cuvettes.

Gel electrophoresis was carried out according to Laemmli (13) either at room temperature or at 4 °C for the gel used for heme peroxidase revelation by Enhanced Chemiluminescence (ECL) (14); in that last case the gel was transferred on a nitrocellulose membrane before development. Amino acid analysis was performed after 6 N HCl hydrolysis for 24 h at 110 °C by the Laboratoire de Chimie Organique at the Institut Pasteur.

Resonance Raman Spectroscopy—Resonance Raman (rR) spectra were obtained from 10 to 55 μM HasA, HasR, and HasA·HasR samples, which were contained in a 5-mm NMR tube spinning at ~20 Hz. Raman scattering was excited using either 413.1 nm emission from a Kr+ laser (10 milliwatt). UV-visible absorbance spectra were recorded before and after the rR experiments to ensure that the samples were not irreversibly altered in the laser beam. No spectral artifacts attributable to laser-induced sample damage were observed. Spectra were recorded at ambient temperature using 135° backscattering geometry with the laser beam focused to a line. Scattered light was collected with an f1 lens and filtered with a holographic notch filter to attenuate Rayleigh scattered light. The polarization of the scattered light was then scrambled, and the spot image was f-matched to a 0.63-m spectrograph fitted with a 2400 groove/mm grating and a LN2-cooled CCD camera. The spectrometer was calibrated using the Raman bands of toluene and *N*,*N*-dimethylformamide as external frequency standards.

Isothermal Titration Calorimetry (ITC)—Titrations were performed at 25 °C using a MicroCal MCS titration calorimeter (MicroCal Inc., Northampton, MA) (15). Proteins and hemin were in 20 mM sodium phosphate at pH 7, 0.08% ZW3−14. Samples were thoroughly degassed before use by stirring under vacuum. All injections were carried out at 3-min intervals. Due to heme adsorption, the calorimeter cell and the micro syringe used for injections were extensively washed after each experiment. The heat of dilution of the ligand was measured either by injecting the ligand into the buffer alone or by injecting more ligand into the cell after saturation. The value obtained was subtracted from the heat of reaction to give the effective heat of binding. Because apoHasR contains some contaminants, all of the ITC control titrations were carried out with membrane preparation not expressing HasR and purified in the same manner at the equivalent concentration of contaminant than that present in apoHasR sample, *i.e.* few 10^{-6} M. No higher signal than that corresponding to the heat dilution of ligand was observed. For the titration experiments the concentrations of wild-type and mutant receptors ranged between 2 and 10 μM, and the ligand was set to 10–20 times this value.

The resulting titration data were analyzed and fitted using the Origin for ITC software package supplied by Microcal to obtain the stoichiometry (n), the dissociation constants (K_d), and the enthalpy (ΔH) changes of binding. For the fit any constraints on the stoichiometry and ΔH were not fixed. ITC titrations of HasR with hemin showed 20% of variation of stoichiometry around 1. This was due to the imprecision in the determination of hemin concentration in the presence of detergent and to the fact that hemin is known to be very dynamic in nature inside micelles (16).

The formation of the complex during the ITC experiment was verified by SDS-PAGE and UV-visible spectroscopy. Analysis of the samples by optical absorbance after the ITC experiments was carried out after removal of excess ligand by filtration using a membrane having a molecular mass cut off of 100 kDa. The same protocol was applied for Raman spectroscopy when needed. Ultrafiltration through a membrane having a molecular mass cut off of 100 kDa passes uncomplexed holoHasA and free heme, thereby allowing them to be separated from the complex.

RESULTS

The HasR Receptor Can Be Isolated in Either the Apo or the Holo Form—The *S. marcescens hasR* gene encoding HasR has been cloned into plasmid pBAD24 to yield pFR2. Membranes from the popc4420(pFR2) strain grown in minimal medium in the presence of arabinose contain a large amount of HasR receptor (Fig. 1*A*, *lane 3*) as compared with control membranes from popc4420(pBAD24) grown under the same conditions (Fig. 1*A*, *lane 2*). Large amounts of this receptor can be purified in the presence of detergent (Fig. 1, *lane 7*) using anion exchange followed by size exclusion chromatography. Purified HasR is essentially in its apo form as evidenced by the absence of heme absorbance features in the UV-visible spectrum (see UV-visible spectrum, Fig. 1*C*, *bottom*) The heme-bound receptor is produced by adding a solution of hemin to the culture medium or to the membrane preparation. The resulting heme-bound protein has a characteristic UV-visible spectrum that is very different from that of free heme in detergent. For control membranes not expressing the receptor, no protein-bound heme was found (not shown). The behavior of the heme-bound form, holoHasR, on an anion exchange column is different from that of apoHasR; thus, holoHasR is readily purified by ion exchange chromatography (Fig. 1*A*, *lane 8*, *cf. lane 7*). HoloHasR retains its heme under conditions of SDS-gel electrophoresis. This has been demonstrated by SDS-gel electrophore-

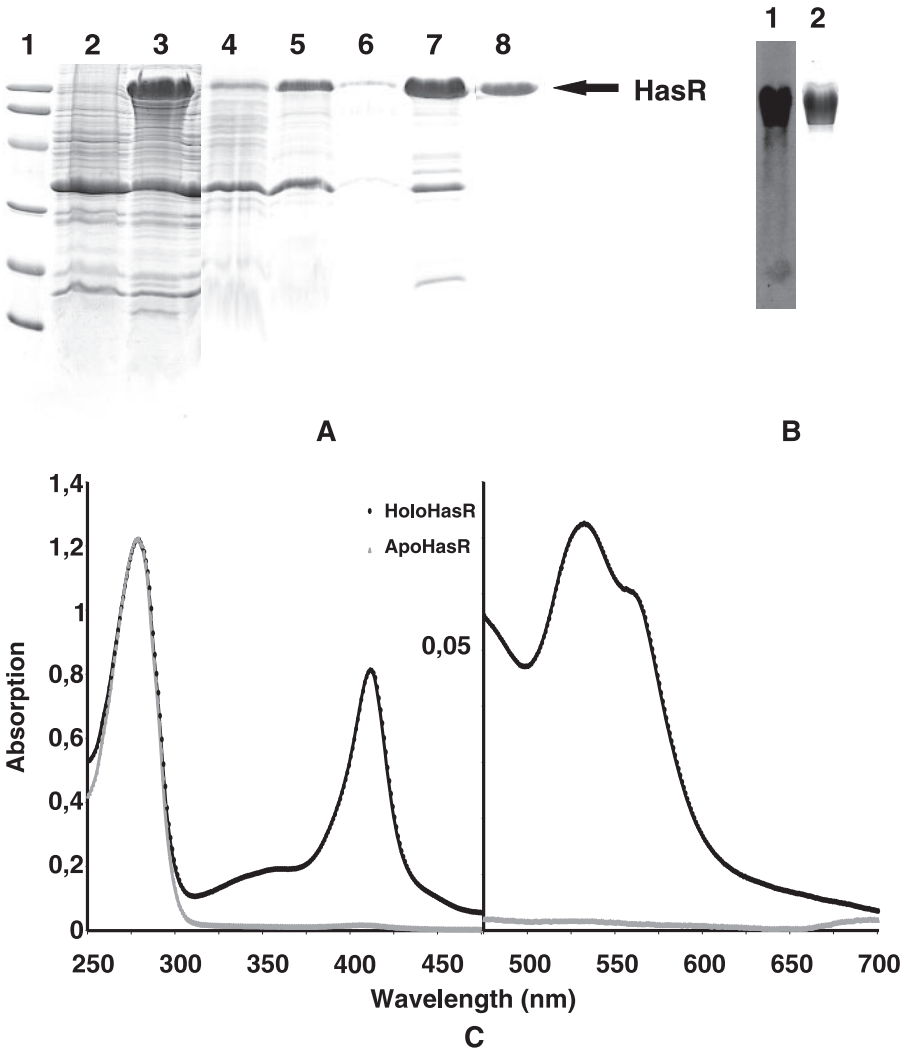

FIGURE 1. **Purification of apo- and holoHasR.** *A*, analysis by gel electrophoresis (14% acrylamide) of whole membranes, solubilization steps, and purified apo- and holoHasR. *Lane 1*, MW markers (92, 66, 45, 31, 21 and 14 kDa); *lane 2*, whole membranes from popc4420(pBAD24); *lane 3*, whole membranes from popc4420(pFR2); *lanes 4–6*, first, second, and third solubilization steps; *lane 7*, partially purified apoHasR; *lane 8*, purified holoHasR. *B*, heme peroxidase activity of purified holoHasR. *Lane 1*, ECL detection; *lane 2*, stained gel of the corresponding sample. *C*, normalized absorption spectra from samples of purified apo- and holoHasR from 250 to 700 nm; the 475–700 nm region is represented with an expanded scale. *Black triangles*, holoHasR; *gray squares*, apoHasR. The spectra were normalized at 278 nm. The Soret band is at 411 nm, and the Q bands are at 532 and 560 nm, respectively.

sis of holoHasR at 4 °C followed by ECL-detected heme peroxidase activity (14) (Fig. 1*B*, *lane 1*).

Purified holoHasR exhibits a characteristic UV-visible spectrum (Fig. 1*C*) having a Soret band at 411 nm and Q bands at 533 and 560 nm. The general appearance of the spectrum is consistent across all preparations. The A_{278}:A_{411} ratio varies between 2 and 1.5 from preparation to preparation depending on the quantity of heme. Amino acid analysis of holoHasR closely matches the HasR amino acid composition (supplemental Table S1). Heme content was quantified by the pyridine-hemochrome method (17), which shows that the heme/HasR mole ratio is essentially 1 (1.06 heme molecule/receptor monomer). The resulting extinction coefficients for holoHasR are 1×10^5 M^{-1} cm^{-1} for the Soret band at 411 nm and 1.5×10^5 M^{-1} cm^{-1} at 278 nm. Accounting for the contribution from heme absorbance at 280 nm, the experimentally determined value for ϵ_{278} is in reasonable agreement with that calculated on the basis of amino acid composition (1.4×10^5 M^{-1} cm^{-1}). Because our apoHasR preparation contains some contaminants, its absorbance in the preparation was estimated to account for ⅔ of the total absorbance at 278 nm. Its concentration in subsequent experiments was estimated using the calculated ϵ_{278} of 1.4×10^5 M^{-1} cm^{-1} and multiplying the result by 2/3.

We have previously shown that both holoHasA and apoHasA bind to cells expressing the HasR receptor. These associations occur with similar affinities and are independent of the TonB complex (5). Herein we address whether analogous behavior occurs between HasA and the purified receptor. Because HasR is purified in the presence of detergent, all of these experiments were carried out in detergent solution to maintain solubility of HasR.

Both ApoHasA and HoloHasA Form a 1:1 Stoichiometric Complex with ApoHasR—Stable complexes form upon mixing of both apo- and holoHasA with apoHasR. These complexes can be isolated chromatographically, but because of impurities in our apoHasR preparations, it was difficult to determine their precise stoichiometries. The impurities, which might account for ⅓ of the absorbance of the apoHasR preparation, do not react with HasA (see ITC section). These impurities cannot, therefore, account for spurious determination of the stoichiometry as we carried it out. A His_6 tag HasA (HisHasA), having the same affinity for heme, spectral characteristics, and competence to deliver heme to the receptor as wild-type HasA (8), was prepared. It was purified to homogeneity in both its holo and apo forms by affinity chromatography. In the presence of apoHasR, a stable HisHasA·HasR complex formed and was separated from HisHasA by a single gel filtration step (Fig. 2, *A* and *B*). Amino acid analyses of HisHasA and HasR complexes made with both apo- and holo-HisHasA were performed. The compositions of both complexes were consistent with 1:1 stoichiometry (supplemental Table S1). It is reasonable to suggest that a similar complex is formed with the non-tagged version of HasA.

UV-Visible Absorbance Spectra of HoloHasR and the Complex Formed between HoloHasA and ApoHasR Are Identical—The absorbance spectrum of the purified complex obtained between holoHisHasA and apoHasR differs markedly from that

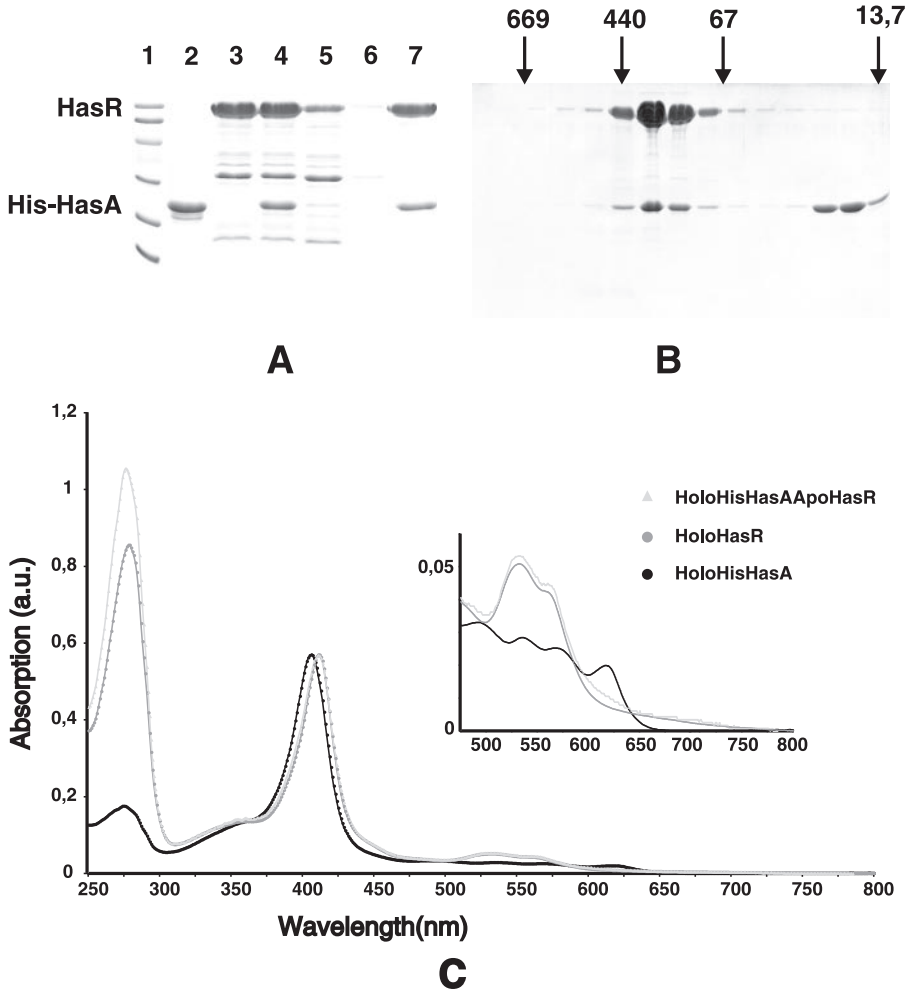

FIGURE 2. **Purification (*A* and *B*) of the HisHasA·HasR complex and UV-visible absorption spectra of holoHisHasA, holoHasR, and holoHisHasA·HasR (*C*).** *A*, affinity purification of apoHisHasA·apoHasR complex and analysis by gel SDS-polyacrylamide gel electrophoresis of different fractions. *Lane 1*, molecular weight markers (92, 66, 45, 31, 21, and 14 kDa); *lane 2*, purified apoHisHasA; *lane 3*, partially purified apoHasR; *lane 4*, apoHisHasA plus apoHasR; *lane 5*, unbound fraction after Ni-NTA affinity chromatography; *lane 6*, wash fraction; *lane 7*, bound fraction after Ni-NTA affinity chromatography. *a.u.*, absorbance units. *B*, gel filtration purification of the apoHisHasA·apoHasR complex after affinity purification. The resulting fraction (*A*, *lane 7*) was run on a Superose 6 column, allowing separation of the complex from free HisHasA. Fractions 23–37 were analyzed by gel electrophoresis. *Numbers* with *arrows above* the gel indicate the position of molecular mass markers in kDa. *C*, absorption spectra of purified holoHisHasA (*black circles*), purified holoHasR (*gray circles*), and purified complex holoHisHasA·apoHasR (*light gray triangles*). The spectra were recorded in 25 mM Tris-HCl, pH 7.5, 150 mM NaCl, 0.02% ZW3-14 and normalized on the Soret band. The 475–800-nm part was expanded.

of holoHasA and is virtually identical to that of holoHasR (Fig. 2*C*). This shows that heme in the HisHasA·HasR complex has an environment similar to that in holoHasR.

To address whether these spectral properties are attributable to the His_6 tag on holoHasA, the spectral changes that occurred upon mixing holoHasA and a 1.5 M excess of apoHasR were monitored. After several minutes no further spectral changes were observed, suggesting that the reaction had reached equilibrium (Fig. 3). The spectral changes included a shift of the Soret band from 406 nm (holoHasA in detergent) to 411 nm (characteristic of holoHasR), the disappearance of the 620-nm band in the holoHasA spectrum, and the shift of the Q bands (537 and 567 nm in holoHasA *versus* 533 and 560 nm in the complex, also characteristic of holoHasR) and increase in intensity. The spectra of both holoHasR and freshly prepared complex between holoHasA and apoHasR are almost indistinguishable after normalization of the Soret bands, showing that heme has similar environments in the WT and His-tagged preparations and that the His tag did not contribute to the spectral shift in the purified complex (Fig. 2). Upon HasA·HasR complex formation, the heme initially bound to HasA changes its environment to one similar to that in holoHasR, consistent with the heme having been transferred from holoHasA to apoHasR.

Resonance Raman Spectra of holoHasR and the Complex Formed between HoloHasA and ApoHasR Are Identical and Differ from That of HoloHasA—As a means of further testing our hypothesis that heme is transferred from HasA to HasR, we have used resonance rR spectroscopy to compare and contrast the heme environments in holoHasR, holoHasA, and the HasA·HasR complex. The vibrational signatures of the heme, which are provided by rR, constitute a sensitive probe of heme structure, conformation, and environment in proteins.

rR spectra were recorded for holoHasA, holoHasR, and the complex formed between holoHasA and apoHasR (Fig. 4). Oxidation state, spin state, and ligation state marker bands for heme proteins are observed in the high frequency region of their rR spectra. Two υ_3 bands (1476 and 1503 cm^{-1}) are observed for holoHasA, consistent with the protein existing in both 6-coordinate high spin and 6-coordinate low spin forms as reported previously (18). Upon the addition of excess apoHasR, the υ_3 band attributed to 6-coordinate low spin heme shifts from 1503 to 1501 cm^{-1}, where it appears in the spectrum of holoHasR. The rR spectrum of this complex is characteristic of ferric 6-coordinate bishistidine complexes. Accordingly, the oxidation state/porphyrin π^* marker band, υ_4, for holoHasA, holoHasR, and the HasA·HasR complex is observed at 1372 cm^{-1}, typical of ferric hemes. A small band at about 1476 cm^{-1} persists after the transfer reaction has reached equilibrium. The spectrum in Fig. 4 is that of a 1:2 mixture of holoHasA and apoHasR. The spectrum of a 1:3 mixture exhibits the same small band. This band persists even after the complex is washed with an excess of buffer via ultra filtration. Hence, the υ_3 band at 1476-cm^{-1} is intrinsic to the complex and corresponds to neither uncomplexed holoHasA nor free heme.

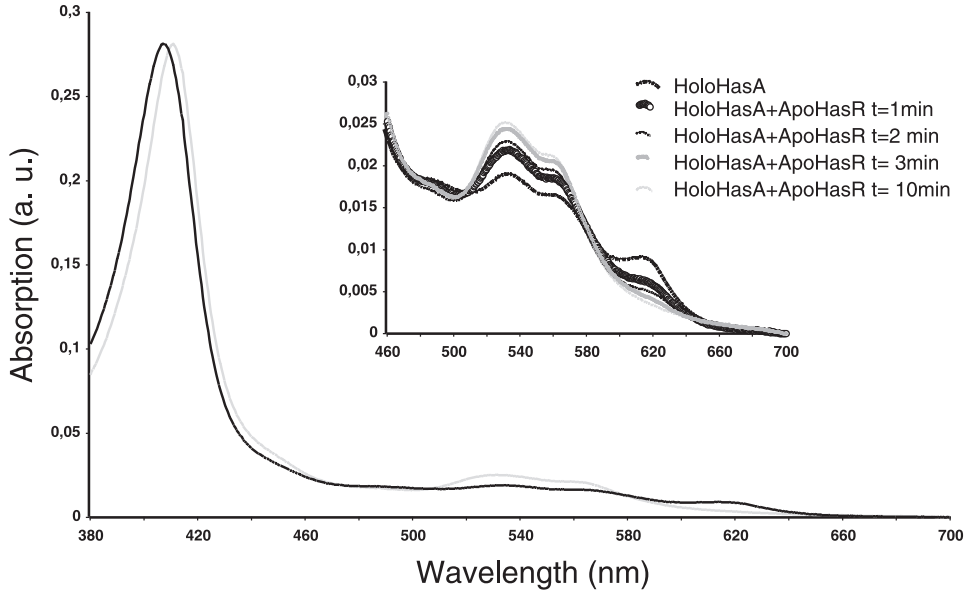

FIGURE 3. **Variation of absorbance upon mixing of holoHasA (3×10^{-6} M) with a molar excess of apoHasR.** Pure holoHasA is shown in *black* and 10 min after mixing with apoHasR (*gray*). The *inset* shows the variation of the absorption spectrum as a function of time upon mixing in the 460–700-nm region. *a.u.*, absorbance units.

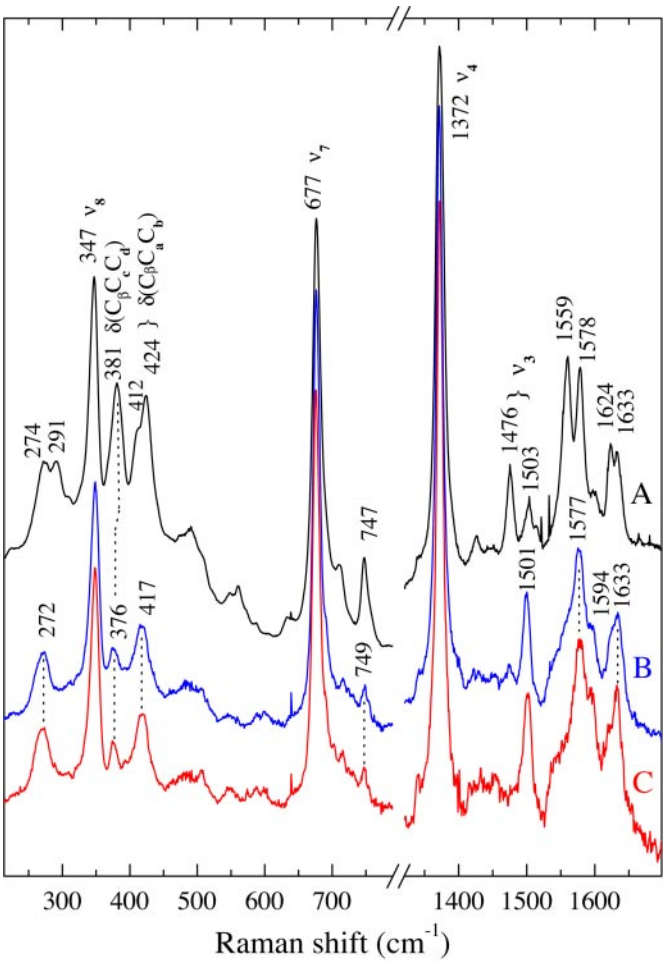

FIGURE 4. **Comparison of the resonance Raman spectra of holoHasA and holoHasR obtained with 413.1-nm excitation.** HoloHasA (*A*) and HasA·HasR (*B*) complex generated by the addition of holoHasA to apoHasR in a 1:2 ratio and HasR loaded with hemin by the addition of hemin in 1:1 ratio (*C*). All samples were in 20 mM sodium phosphate, pH 7, 0.08% ZW.

The bending modes observed for the peripheral heme propionate $\delta(C_\beta C_c C_d)$ and vinyl $\delta(C_\beta C_a C_b)$ groups in holoHasR have been tentatively assigned to the bands at 376 and 417 cm^{-1} by comparison with rR assignments for bisimidazole heme model complexes and proteins (19, 20). Moreover, the low frequency rR spectra of holoHasR and the HasA·HasR complex are indistinguishable. Thus, the propionate and vinyl substituents of the hemes in authentic holoHasR and in the HasA·HasR complex are in comparable environments.

Given that (*a*) the heme in holoHasA exists as an equilibrium mixture of high and low spin states and (*b*) the heme in authentic holoHasR is completely low spin, there are two possible explanations for the features in the rR spectrum of the HasA·HasR complex. One is that the heme remains associated with HasA when it complexes with apoHasR, and it is the protein-protein interaction that drives the spin state change to convert all the heme to a low spin form. The second explanation is that the heme is transferred from holoHasA to HasR upon protein-protein complexation. The latter is supported by the identity between the rR signatures of holoHasR and the HasA·HasR complex. The aforementioned similarities in both the axial ligand field and peripheral heme environment constitute compelling circumstantial evidence that heme is transferred from its binding site in HasA to a binding site in HasR upon complex formation.

ITC Studies of the Interaction of HasR with Its Different Ligands, Heme/ApoHasA/HoloHasA—We have used isothermal titration calorimetry to understand the molecular events involved in this transfer and to characterize the interaction between the three partners, HasA, HasR, and heme.

HasR/Heme—the ITC titration of apoHasR with hemin displays a very weak enthalpic signal. The data fit to a single-site (or set of equivalent sites) model with a stoichiometry close to 1, an affinity constant of $5(\pm 3) \times 10^6$ M^{-1}, and a ΔH of -18 ± 3 kJ·mol^{-1} (Table 1). Because the apoHasR preparations were not pure, a control experiment on similar preparation from a strain that does not express HasR was carried out. No signal apart from that attributable to dilution was detected.

ApoHasA/Heme—This has already been studied in detail (4). ITC titration of heme binding to HasA in the presence of detergent shows that the detergent does not perturb the interaction; ΔH is -105 kJ·mol^{-1}, and the affinity constant is $>10^9$ M^{-1}. In addition, the structural fingerprints of ^{15}N-labeled holoHasA in 20 mM sodium phosphate buffer, pH 7, with or without detergent have been compared by ^{1}H,^{15}N heteronuclear single quantum correlation spectrum. These spectra are identical, showing that the presence of detergent does not modify the holoHasA structure (data not shown).

TABLE 1

Affinity constants, stoichiometries, and Δ*H* of binding of wild-type HasR with hemin, apoHasA, and holoHasA and of HasRH1H2 with apoHasA at 25 °C in 20 mM sodium phosphate, pH 7, in the presence of 0.08% ZW 3–14

K_{obs} and ΔH_{obs} are the values obtained by fitting the ITC data and reflect that of binding + heme transfer.

Binding partners	*n*	K_a	Δ*H*
		M^{-1}	$kJ{\cdot}mol^{-1}$
ApoHasR + heme	1.07 ± 0.15	5 (±3) 10^6	−18 ± 3
ApoHasA + heme	1.05 ± 0.02	5.3 (±1.6) 10^{10}	−105.4 ± 3.8
ApoHasR + apoHasA	0.98 ± 0.01	$>10^9$	−201 ± 1.6
ApoHasA + apoHasRH1H2	1.01 ± 0.01	3 (±0.5) 10^7	−136 ± 1.3
ApoHasR + holoHasA	1.06 ± 0.02	K_{aobs} = 4.9 (±1.8) 10^7	ΔH_{obs} = −105 +/−3

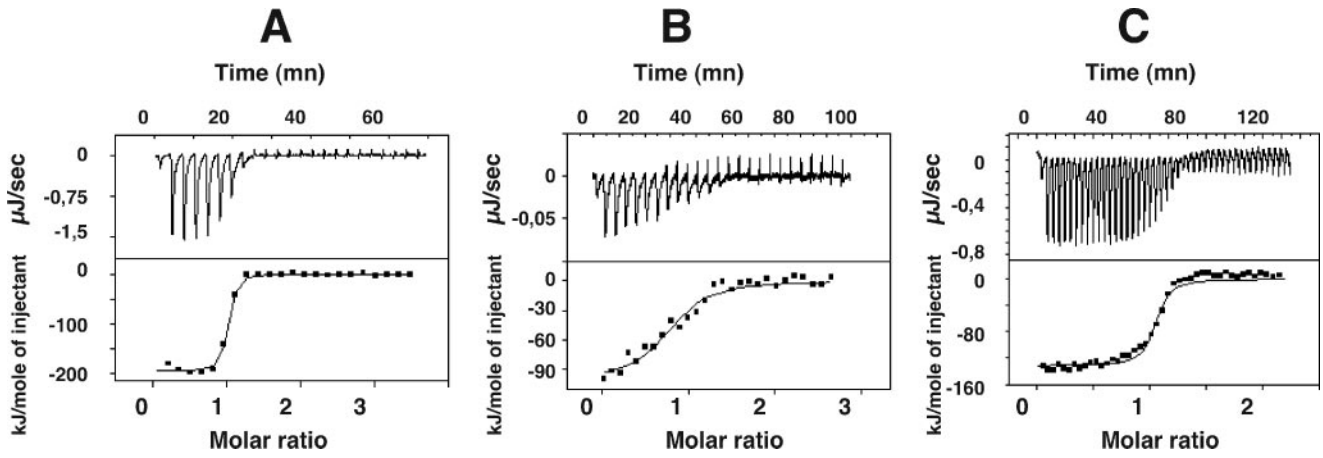

FIGURE 5. **ITC analysis of the interaction of apoHasA and apoHasR (*A*), holoHasA and apoHasR (*B*), and apoHasA and apoHasRH1H2 (*C*).** Representative experiments are shown. In each case the heat signal is shown (*upper*) together with the binding isotherm derived from this signal (*lower*).

ApoHasA/ApoHasR—ITC titration of apoHasR with apoHasA gave very strong negative enthalpic signals. The data fit to a single-site model with a 1:1 stoichiometry, a Δ*H* of −201 ± 16 $kJ{\cdot}mol^{-1}$, and an affinity constant $>10^9$ M^{-1}, too large to be deduced precisely from ITC titration (Fig. 5*A*). Whatever the exact value, it shows the very high affinity of the receptor for the hemophore, which is at least 10-fold higher than the apparent K_a estimated *in vivo*. Again there was no signal with the control preparation, showing the specificity of the signal.

HoloHasA/ApoHasR—The ITC titration of apoHasR by holoHasA gave an enthalpic signal lower than that observed for apoHasA-apoHasR (Fig. 5*B*). Fitting of the data by a single-site model indicated a 1:1 stoichiometry and an observed enthalpy change (ΔH_{obsd}) of −105 $kJ{\cdot}mol^{-1}$. The UV-visible spectral properties of the complex so formed after removal of the excess of ligand shows that heme transfer accompanies the formation of the complex from holoHasA to apoHasR. The observed ITC signal is, thus, the sum of the protein-protein interaction signal, that of extracting heme from HasA and that of transferring heme to apoHasR. Hence, the observed enthalpy signal varies on the basis of the equation $\Delta H_{obsd} = \Delta H_{binding} - \Delta H_{heme\text{-}HasA} + \Delta H_{heme\text{-}HasR}$. Hence, $\Delta H_{binding} = \Delta H_{obsd} + \Delta H_{heme\text{-}HasA} - \Delta H_{heme\text{-}HasR} = -105\ kJ{\cdot}mol^{-1} - 105\ kJ{\cdot}mol^{-1} + 18\ kJ{\cdot}mol^{-1}$, and the $\Delta H_{binding}$ of holoHasA to apoHasR given by this equation is −192 $kJ{\cdot}mol^{-1}$. This value is comparable with that obtained by ITC for the binding of apoHasA and apoHasR (−201 $kJ{\cdot}mol^{-1}$). No difference was found for *in vivo* binding of both forms of HasA to HasR, and no structural difference was observed in the regions of HasA shown to be involved in interaction with HasR in the presence or in the absence of heme.[4] All those results are consistent with the fact that the same polar interactions are involved in the binding of both forms of HasA (apo/holo) to HasR. The interaction of HasA with HasR involves two distinct β strands on HasA, and the very large Δ*H* value suggests that several residues are involved in the interaction.

The exact K_a between holoHasA and apoHasR cannot be directly measured by ITC titration because of the heme transfer reaction occurring during the ITC measurement. The apparent K_a between holoHasA and apoHasR is in the order of 5×10^7 M^{-1}.

Role of the Two Conserved HasR Histidine in Heme Uptake and Heme Transfer from HasA to HasR—To gain further insight into the heme transfer reaction between holoHasA and apoHasR, both HasR and HasA mutants were constructed and studied *in vivo* and *in vitro*. Like many heme receptors, HasR contains two conserved histidine residues, one in the plug His-189 (hereinafter referred to as H1) and the other one in the β-barrel His-603 (hereinafter referred to as H2). Mutation of these residues in HemR, the heme receptor from *Y. enterocolitica* or HmuR from *Porphyromonas gingivalis*, led to an inactive receptor (9, 21). Homology modeling of HasR using the already crystallized receptors structures as templates indicated that those two residues might be in close proximity at the apex of the receptor, H1 at the top of the plug and H2 in an extracellular loop and facing the plug (8). Both were mutagenized into

[4] N. Wolff, N. Izadi-Pruneyre, J. Couprie, M. Habeck, J. Linge, W. Rieping, C. Wandersman, M. Nilges, M. Delepierre, and A. Lecroisey, manuscript in preparation.

TABLE 2

Growth around wells of C600Δ*hemA* producing either wild-type HasR receptor or HasRH1, HasRH2, and HasRH1H2 expressed from pFR2 plasmid and mutants thereof in the presence of different heme sources

No growth was observed with the C600Δ*hemA exbBD*::*Tn10* strain. Arabinose concentration was 20 mg/liter; dipyridyl concentration was 0.2 mM. HasA wild-type and mutants were heme-loaded at 80% saturation, and the concentration refers to the heme-loaded part. ++++, growth around the well of around 8 mm; +++, growth around the well of around 5 mm; +, growth around the well of around 2 mm; −, no growth around the well. NT, not tested; NA, not applicable.

Heme source	Heme affinity	HasRWT	HasRH2	HasRH1	HasRH1H2
HasA, 40 μM	5.3×10^{10} M^{-1}	++++	−	−	−
HasA76t, 40 μM	7×10^{8} M^{-1}	−	NT	NT	NT
HasA76t, 4 μM	7×10^{8} M^{-1}	−	NT	NT	NT
Heme, 40 μM	NA	++++	+	+−	−
Heme, 4 μM	NA	+	−	−	−
Hemoglobin, 40 μM	?	++++	−	−	−
Hemoglobin, 4 μM	?	+	−	−	−
HasA, WT, 40 μM	5.3×10^{10} M^{-1}	++++	−	−	−
H32A, 40 μM	10^{10} M^{-1}	++++	−	−	−
H83A, 40 μM	2×10^{8} M^{-1}	++++	++++	−	−
Y75A, 40 μM	10^{8} M^{-1}	++++	++++	−	−
H32A,H83A, 40 μM	2.3×10^{7} M^{-1}	++++	++++	−	−
Y75A,H83A, 40 μM	1.8×10^{6} M^{-1}	++++	++++	++++	−
H32A,Y75A, 40 μM	6×10^{4} M^{-1}	++	++	++	−

alanine and the two single mutants, and the double mutants were constructed. All three proteins were expressed to comparable levels without evidence for degradation. They were correctly localized to the outer membrane and shown by dot-blot to interact with HasA (data not shown). All three proteins could be purified using the same protocol as for wild-type apoHasR, and the same molar extinction coefficient values were used to estimate their concentrations.

In vivo experiments indicated that both single mutants were still able to take up free heme but with a lower efficiency than the wild-type receptor, whereas the double mutant was no longer able to take up free heme (Table 2). This heme uptake was TonB complex-dependent (not shown). This indicates that one of the two histidines is sufficient to bind and internalize heme, but higher heme concentration than that necessary for WT-receptor was required for growth. This suggests that the affinity of these receptors for heme is affected by the mutation. The ITC titration of these simple mutants with hemin in our experimental conditions did not show higher enthalpic signal than that of dilution. This is compatible with the loss of one iron coordination and the very weak enthalpic signal observed for the wild-type receptor with heme. It is expected that the double mutant has no significant affinity for heme.

Although holoHasA could not be used as a heme source by any of the mutants (Table 2), ITC experiments indicated that all mutants were able to form 1:1 complexes with holoHasA and apoHasA, as does wild-type HasR. The absorbance spectra of the complexes formed were all similar to HasA spectra (data not shown). ITC showed that the interaction of the double mutant receptor with HasA is different from that of apoHasA-apoHasR: ΔH of binding of apoHasA·HasRH1H2 is lower (-136 kJ·mol^{-1} *versus* -210 kJ·mol^{-1} for apoHasA-apoHasR), and the affinity constant is 3×10^{7} M^{-1}, whereas that of the interaction of apoHasA with the wild-type receptor is $>10^{9}$ M^{-1} (Table 1, Fig. 5*C*). This significant difference in binding, which could be attributable to structural modifications of this mutant or at least of the parts of the receptor involved in the binding with HasA, precluded further analysis of the heme transfer from thermodynamic parameters.

HasRH1 and HasRH2 mutants are still active heme transporters but cannot acquire heme from wild-type HasA. If the heme transfer step from HasA to HasR depends upon the respective affinities of HasA and HasR for heme, one might then expect that HasA mutants having lower heme affinities (mutated in the three residues involved in the heme axial ligation His-32, Tyr-75, and His-83) could still serve as heme sources for the HasR mutants studied here, since none of them are *per se* required for heme transport. Hence, the abilities of these HasA heme pocket mutants to serve as heme sources for the WT and mutant receptors were explored. The results of these experiments are shown in Table 2. Under our conditions, the wild-type receptor can use HasA wild type and the mutants tested whose affinity for heme ranges from 5.3×10^{10} M^{-1} to 6×10^{4} M^{-1}. Whereas neither wild-type HasA ($K_a = 5.3 \times 10^{10}$ M^{-1}) nor HasA-H32A ($K_a = 1 \times 10^{10}$ M^{-1}) can serve as an heme source for the H2 mutant of the receptor, all the other HasA mutants with lower affinities starting with HasA-H83A ($K_a = 2 \times 10^{8}$ M^{-1}) could. A similar situation was found with the H1 mutant where none of the HasA mutants could serve as the heme source except HasA-Y75A-H83A ($K_a = 1.8 \times 10^{6}$ M^{-1}) and HasA-H32A-Y75A ($K_a = 5.9 \times 10^{4}$ M^{-1}). Our results indicate that the mutation of one of the two histidines does not abolish the capacity of HasR to acquire heme either free or bound to HasA but only decreases it. Moreover the two histidines are not equivalent since the mutation of H2 (barrel histidine) results in a milder defect in heme acquisition as compared with that of H1 (plug histidine). Hence, it is concluded that the two histidines are responsible for heme fixation of the receptor and are not equivalent in the functioning of the receptor.

DISCUSSION

Heme transfer between hemophore and its receptor is a peculiar case of prosthetic group transfer for scarce, yet necessary compounds that are internalized by a cell, in this case to fulfill its iron needs. As a consequence of scarcity, the first binding step has to be of high affinity, as is the case for siderophores (22, 23). The release step has been solved in different ways. In higher eukaryotes in the case of transferrin its extremely high affinity for iron is regulated by the surrounding pH, and upon transferrin receptor/transferrin internalization and acidification in lysosomes iron is released from transferrin. Apotransferrin and receptor are then recycled at the cell surface (1).

Bacteria using transferrin or hemoproteins (*i.e.* very high affinity binding sites for their prosthetic groups) as an iron source have to solve this problem at the extracellular surface, and this question has not yet been addressed in molecular terms (24, 25). In the case of outer membrane receptors for siderophores, the binding site is of high affinity and exposed to the extracellular medium, whereas the next partner the binding protein resides in the periplasm and has a lower affinity for its substrate than the receptor. In the Fep system, for example, the periplasmic binding protein has a 300 times lower affinity for enterobactin than the outer membrane receptor (26). Both the thermodynamically unfavorable drop in affinity and the topologically different locations are compensated for by the role of the proton motive force, and the TonB complex functions to allow access to the periplasmic space for the substrate and either directly or indirectly allows a drop in affinity such that transfer to the binding protein is favored. It has been proposed that upon action of the TonB complex, the plug is physically ejected from the barrel and pulls the substrate into the periplasmic space (27). This hypothesis, although very attractive, has not yet received strong experimental support.

HasR is one such outer membrane receptor involved in heme transport across the outer membrane. This heme transport process is an active one since it involves the TonB complex and the proton-motive force across the inner membrane (11). Although HasR transports only heme, it is able to recognize three substrates from the extracellular side, either free heme or apo or holohemophore. In the case of heme uptake from the hemophore, the TonB complex is required both at the heme transport step across the outer membrane through the receptor and at the dissociation of the empty hemophore from the receptor. The latter step is the most energy-consuming (11).

In this study we showed that HasR binds one molecule of heme with an affinity of 5×10^6 M^{-1}. In holoHasR, the Raman and UV-visible spectral signatures are consistent with bishistidine axial ligation of a low spin heme iron. Individual mutation of the two conserved histidines in HasR decreases its capacity for heme acquisition, thereby establishing His-189 in the plug and His-603 in the barrel as heme ligands in HasR. The affinity of HasR for heme is much lower than the affinity of siderophores for their cognate receptors and is consistent with our *in vivo* observations of growth stimulation by heme of a heme auxotroph strain expressing the HasR receptor. However, the affinity for heme of HasR is on the same order as that of other heme receptors. The present study shows that HasR forms stable 1:1 complexes with both the apo and holo forms of HasA with affinities $>10^9$ M^{-1}. This makes the heme acquisition by HasR via HasA very efficient and advantageous compared with the heme receptors of other bacteria.

The most striking result of our study is that heme transfers from purified holoHasA to apoHasR *in vitro* in the absence of any source of energy external to the HasA·HasR complex. This transfer of heme is supported by several independent lines of evidence. Changes in the UV-visible and rR spectra are consistent with formation of a new bis-His-ligated heme having a peripheral heme environment distinct from that in holoHasA. The thermodynamic parameters of interaction between holoHasA and apoHasR, as compared with those of the self-association of the individual components and their association with heme, are consistent with this conclusion. These lines of evidence suggest that the protein-protein interaction between HasA and HasR drives heme transfer despite the unfavorable difference of affinity for heme. Analysis of HasA·HasR complexes obtained with mutants of both HasA and HasR also corroborated this conclusion.

Such phenomena may also occur in other receptors that recognize heme or iron-containing proteins, and a reasonable hypothesis is that substrate transfer will be spontaneous due to protein-protein interaction and independent of TonB. In this respect, it should be mentioned that apo and holo human transferrin recognize the *Neisseria* transferrin receptor TbpA *in vitro* and that the ΔH is much lower for holoTf than for apoTf (28). The lower ΔH seen for holoTf-TbpA may be the result of a protein-protein interaction and of the extraction of iron from transferrin and of its binding to the receptor. However, iron transfer from transferrin ($K_a = 10^{18}$ M^{-1}) to the receptor has not been studied either *in vivo* or *in vitro* (29). It has been proposed that bilobate structures might provide adequate environment for such binding and release of cofactors, in particular in the case of transferrin or hemopexin (30). In the HasA case, the contribution of the polar interactions in the binding process between HasA and HasR seems to be equivalent and heme-independent. In any case, the HasA structure might also be well adapted for binding and release of the cofactor. In HasA, heme is coordinated by the N_ϵ of His-32 on one side and by the O_η of Tyr-75 on the other side. These two residues and a third, His-83, which play important roles in the binding of heme, are located on two loops separated by three β strands, one of which contains a binding site for HasR (7). Furthermore, the structural organization of HasA places one of the β strands involved in interaction with HasA less than 10 Å from each of the heme ligands. These spatial relationships between the heme and HasR binding sites of HasA may facilitate the propagation of local conformational changes driven by the HasA·HasR interaction to the heme ligands of HasA and promote the heme delivery from HasA to HasR. In this respect it is worth mentioning that a HasA mutant isolated during the course of a systematic pentapeptide insertion mutagenesis (7) bore an insertion at position 76 close to Tyr-75, one of the heme ligands. This mutant (HasA76t) is able to bind heme with high affinity ($K_a = 7 \times 10^8$ M^{-1}) and is able to bind to the receptor, as shown by dot-blot analysis on intact cells expressing the receptor (31), but is unable to serve as a heme source for the wild-type receptor. *In vitro* with purified apoHasR, HasA76t makes complexes comparable with the wild-type HasA but without the characteristic spectral changes, suggesting that heme is not transferred to HasR. The insertion of this pentapeptide in mutant HasA76t at position $n + 1$ in the loop containing Tyr-75 heme ligand seems to inhibit whatever conformational reorganization is normally induced by HasR and required for heme transfer. Nevertheless, the binding of HasA to HasR seems to be irreversible *in vitro*, consistent with the fact that ejection of apoHasA requires energy provided by the TonB complex. This suggests that some structural changes of HasR and/or HasA should occur to allow the dissociation. Moreover, attempts to dissociate the complex *in vitro* at high ionic strength chemically

or thermally have so far been unsuccessful. The sites of interaction between HasA and HasR have been defined on HasA (7), and one expects that definition of those sites on HasR will help understanding the heme transfer process as well as the ejection of hemophore under the action of the TonB complex.

A similar movement of cofactor/substrate upon protein-protein interaction has been reported for ADP/phosphate release upon interaction of myosin and actin, where the closing of the actin binding cleft is coupled to the opening of the nucleotide binding pocket (32). Although it is reasonable to suspect that heme transfer reactions similar to that reported here would be common, heme transfer that is apparently driven by protein-protein interaction has only been described for the heme transport systems of *Pseudomonas aeruginosa* (33) and *Streptococcus pyogenes* (34). Among the systems studied to date, HasA/HasR is unique in that its thermodynamic parameters are well quantified. This system is, therefore, well suited for elucidating further details of the thermodynamic and structural bases of the mechanism by which heme is transferred between these proteins.

Acknowledgments—Some ITC experiments were performed at the biophysical platform of Institut Pasteur directed by Patrick England. We thank Sylviane Hoos for technical assistance. We thank Muriel Delepierre for constant interest in this work and our colleagues Sylvie Létoffé, Francis Biville, and Laurent Debarbieux for helpful discussions during this work.

REFERENCES

1. Hentze, M. W., Muckenthaler, M. U., and Andrews, N. C. (2004) *Cell* **117,** 285–297
2. Ferguson, A. D., and Deisenhofer, J. (2004) *Cell* **116,** 15–24
3. Wandersman, C., and Delepelaire, P. (2004) *Annu. Rev. Microbiol.* **58,** 611–647
4. Deniau, C., Gilli, R., Izadi-Pruneyre, N., Létoffé, S., Delepierre, M., Wandersman, C., Briand, C., and Lecroisey, A. (2003) *Biochemistry* **42,** 10627–10633
5. Létoffé, S., Deniau, C., Wolff, N., Dassa, E., Delepelaire, P., Lecroisey, A., and Wandersman, C. (2001) *Mol. Microbiol.* **41,** 439–450
6. Arnoux, P., Haser, R., Izadi, N., Lecroisey, A., Delepierre, M., Wandersman, C., and Czjzek, M. (1999) *Nat. Struct. Biol.* **6,** 516–520
7. Létoffé, S., Debarbieux, L., Izadi, N., Delepelaire, P., and Wandersman, C. (2003) *Mol. Microbiol.* **50,** 77–88
8. Létoffé, S., Wecker, K., Delepierre, M., Delepelaire, P., and Wandersman, C. (2005) *J. Bacteriol.* **187,** 4637–4645
9. Bracken, C. S., Baer, M. T., Abdur-Rashid, A., Helms, W., and Stojiljkovic, I. (1999) *J. Bacteriol.* **181,** 6063–6072
10. Létoffé, S., Ghigo, J. M., and Wandersman, C. (1994) *Proc. Natl. Acad. Sci. U. S. A.* **91,** 9876–9880
11. Létoffé, S., Delepelaire, P., and Wandersman, C. (2004) *J. Bacteriol.* **186,** 4067–4074
12. Izadi, N., Henry, Y., Haladjian, J., Goldberg, M. E., Wandersman, C., Delepierre, M., and Lecroisey, A. (1997) *Biochemistry* **36,** 7050–7057
13. Laemmli, U. K. (1970) *Nature* **227,** 680–685
14. Vargas, C., McEwan, A. G., and Downie, J. A. (1993) *Anal. Biochem.* **209,** 323–326
15. Wiseman, T., Williston, S., Brandts, J. F., and Lin, L. N. (1989) *Anal. Biochem.* **179,** 131–137
16. Maiti, N. C., Mazumdar, S., and Periasamy, N. (1995) *J. Phys. Chem.* **99,** 10708–10715
17. Berry, E. A., and Trumpower, B. L. (1987) *Anal. Biochem.* **161,** 1–15
18. Caillet-Saguy, C., Delepierre, M., Lecroisey, A., Bertini, I., Piccioli, M., and Turano, P. (2006) *J. Am. Chem. Soc.* **128,** 150–158
19. Hurst, J. K., Loehr, T. M., Curnutte, J. T., and Rosen, H. (1991) *J. Biol. Chem.* **266,** 1627–1634
20. Choi, S., and Spiro, T. G. (1983) *J. Am. Chem. Soc.* **105,** 3683–3692
21. Liu, X., Olczak, T., Guo, H. C., Dixon, D. W., and Genco, C. A. (2006) *Infect. Immun.* **74,** 1222–1232
22. Schalk, I. J., Hennard, C., Dugave, C., Poole, K., Abdallah, M. A., and Pattus, F. (2001) *Mol. Microbiol.* **39,** 351–360
23. Annamalai, R., Jin, B., Cao, Z., Newton, S. M., and Klebba, P. E. (2004) *J. Bacteriol.* **186,** 3578–3589
24. Gray-Owen, S. D., and Schryvers, A. B. (1996) *Trends Microbiol.* **4,** 185–191
25. Retzer, M., Yu, R., and Schryvers, A. (1999) *Mol. Microbiol.* **32,** 111–121
26. Sprencel, C., Cao, Z., Qi, Z., Scott, D. C., Montague, M. A., Ivanoff, N., Xu, J., Raymond, K. M., Newton, S. M., and Klebba, P. E. (2000) *J. Bacteriol.* **182,** 5359–5364
27. Usher, K. C., Ozkan, E., Gardner, K. H., and Deisenhofer, J. (2001) *Proc. Natl. Acad. Sci. U. S. A.* **98,** 10676–10681
28. Krell, T., Renauld-Mongenie, G., Nicolai, M. C., Fraysse, S., Chevalier, M., Berard, Y., Oakhill, J., Evans, R. W., Gorringe, A., and Lissolo, L. (2003) *J. Biol. Chem.* **278,** 14712–14722
29. Cornelissen, C. N. (2003) *Front. Biosci.* **8,** 836–847
30. Paoli, M., Anderson, B. F., Baker, H. M., Morgan, W. T., Smith, A., and Baker, E. N. (1999) *Nat. Struct. Biol.* **6,** 926–931
31. Cwerman, H., Wandersman, C., and Biville, F. (2006) *J. Bacteriol.* **188,** 3357–3364
32. Holmes, K. C., Angert, I., Kull, F. J., Jahn, W., and Schroder, R. R. (2003) *Nature* **425,** 423–427
33. Lansky, I. B., Lukat-Rodgers, G. S., Block, D., Rodgers, K. R., Ratliff, M., and Wilks, A. (2006) *J. Biol. Chem.* **281,** 13652–13662
34. Liu, M., and Lei, B. (2005) *Infect. Immun.* **73,** 5086–5092